Distinctive characteristics of electromagnetic force distributions in compressed plasma flows

Y.E.Volkova[2], D.G. Solyakov[1,2], T.M. Merenkova[1], I.E. Garkusha[1,2], M.S. Ladygina[1], A.K. Marchenko[1], Yu.V. Petrov[1], V.V. Chebotarev[1], V.A. Makhlai[1], V.V. Staltsov[1], D.V. Yeliseyev[1]

[1] *Institute of Plasma Physics, NSC "Kharkiv Institute of Physics and Technology", Kharkiv, Ukraine*

[2] *V.N. Karazin Kharkiv National University, Kharkiv, Ukraine*

The experiments have been recently carried out in the MPC facility. Three gases were used at different initial concentrations. Spatial distributions of the Ampere force have been plotted by using the data retrieved from the magnetic probe measurements. The results have clearly shown that the peculiarities of the compressive structures where the force is directed mainly to the near-axis region or/and opposite to the plasma flow are intrinsically related to specific operating modes. Plasma velocity and density measurements conducted earlier, which illustrate dynamics of the plasma stream deceleration and formation of the compression zone with the average electron density above 10^{18} cm^{-3}, are in agreement with obtained distributions of the local Ampere force.

Introduction

A compression zone is one of the most interesting phenomena inherent in compressive plasma flows. It is formed near the axis of the plasma stream that flows beyond the accelerating channel and compresses in the radial direction. Density and temperature are considerably higher there than in the other parts of the plasma volume [1-7], reaching above 10^{18} cm^{-3} and 60 eV [2-6], respectively. A magnetoplasma compressor (MPC) is a plasmadynamic device generating quasi-steady-state compressive plasma flows [1-11]. Streams of plasma are accelerated towards the axis of the system by the pressure of the azimuthal magnetic field H_φ produced by the current that flows in the discharge plasma. The typical discharge duration is approximately tens of microseconds, which corresponds to the first half-period of the discharge current [2-9].

At present, one of the most crucial research problems is to determine the conditions for the practical use of the MPC for various applications such as lithography or surface modification [4-7]. In this domain, the MPC can serve as an artificial source of extreme ultraviolet

radiation (EUV) [6]. During the experiments with xenon, it has been repeatedly registered with a wavelength of 13.5 nm [2-3, 6]. Among the factors determining the utility of the compressive plasma flows for these purposes, the most essential are the linear size of the compression zone, its spatial location, and the initial concentration of gases used for plasma generation. By taking those into account, it is possible to mitigate the surface erosion of the electrodes caused by the impact of dense and high-temperature plasmas in the compression zone.

It has been shown [2-5, 7-9] that when the initial gas concentration is lowered, not only the linear size of the compression zone rises but also the plasma density in the compression zone goes up. Under those conditions, the compression zone shifts from the electrodes of the plasmodynamic device; thus, the electrode system deteriorates less severely. The theory [1] confirms the results obtained in [2-9]. Figure 1 illustrates how the maximum value of the electron density in the compression zone depends on the initial concentration of working gases. Noticeably, the theoretical curve obtained from Bernoulli's equation [1] coincides with the experimental data, which proves the experimental outcomes to be accurate. Therefore, having selected proper initial conditions, one can ensure that the erosion of the electrodes diminishes.

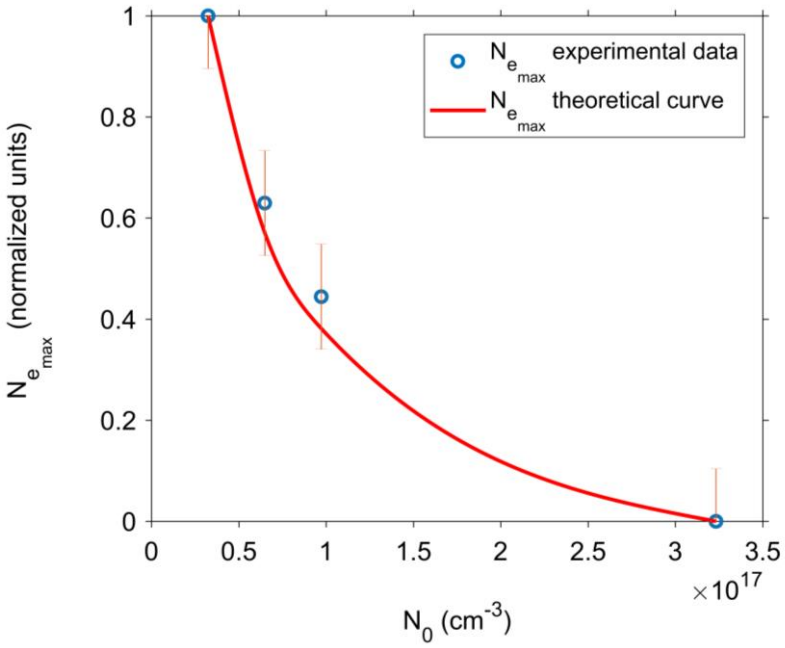

Figure 1: the maximum value of the electron density calculated from the quadratic Stark broadening of spectral lines is compared to the theoretical curve

The research has been carried out using the MPC experimental device [2-9]. We measured a self-generated magnetic field in the plasma streams under different initial experimental conditions, namely varying initial concentrations of gases: helium (33×10^{16} cm^{-3}), nitrogen (2×10^{16} cm^{-3} and 10^{16} cm^{-3}), and argon (3.3×10^{16} cm^{-3}). Assuming a cylindrical symmetry of the system, the spatial distributions of the Ampere force for the indicated operating modes

were calculated and analyzed. With the aid of this approach, it is possible to elucidate the behavior of the plasma flows further [2-3].

Spatial distributions of Ampere force in plasma flows

The spatial distribution of the Ampere force for varying initial concentrations were plotted. The diagrams presented below (Fig. 2 - Fig. 7) depict the direction of the Ampere force at each point of the measurements (vectors), including the region in the proximity of the compression zone. These vectors do not represent the magnitude of the force; however, they indicate how the force is exerted on different parts of the plasma stream. The electrodes (the outer one is an anode) comprising the MPC accelerating channel are shown schematically.

For the smallest initial concentration (up to 2×10^{16} cm^{-3} of nitrogen gas), there is a clearly defined zone where the Ampere force is directed to the axis of the plasma flow. This may correspond to the process of plasma squeezing; thereby, the compression zone forms.

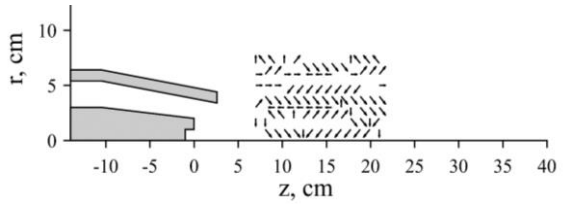

Figure 2: spatial distribution of the Ampere force for the mode of operation with nitrogen ($n_0 \approx 10^{16}$ cm^{-3}). Discharge time 14 μs

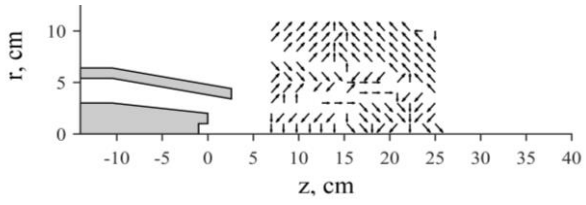

Figure 3: spatial distribution of the Ampere force for the mode of operation with nitrogen ($n_0 \approx 2\times10^{16}$ cm^{-3}). Discharge time 15 μs

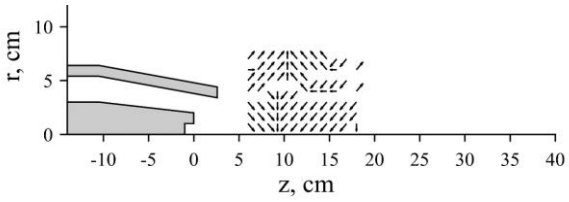

Figure 4: spatial distribution of Ampere force for the mode of operation with argon ($n_0 \approx 3.3\times10^{16}$ cm^{-3}). Discharge time 15 μs

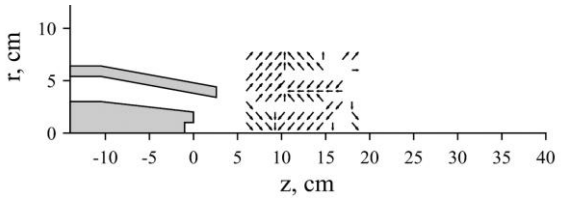

Figure 5: spatial distribution of Ampere force for the mode of operation with argon ($n_0 \approx 3.3\times10^{16}$ cm^{-3}). Discharge time 20 μs

The distribution differs for a slightly higher initial concentration (Fig. 4 and Fig. 5), showing a greater plasma volume involved in the compression process surrounding the axis. According to the detailed analyses of the Bernoulli's equation [1-5], the kinetic energy of a plasma flow transforms into the thermal energy of the compression zone, whereas its velocity decreases.

Since the Ampere force has a longitudinal component in the direction opposite to the plasma stream velocity, a deceleration process occurs.

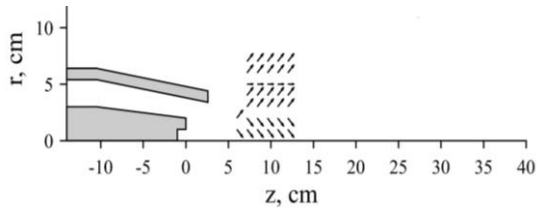

Figure 6: spatial distribution of Ampere force for the mode of operation with helium ($n_0 \approx 33\times10^{16}$ cm^{-3}). Discharge time 8 μs

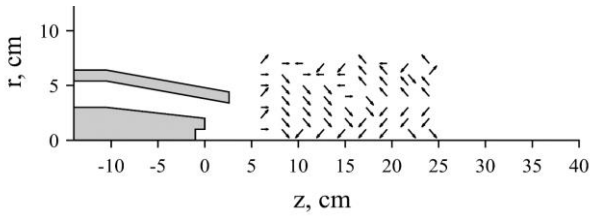

Figure 7: spatial distribution of Ampere force for the mode of operation with helium ($n_0 \approx 33\times10^{16}$ cm^{-3}). Discharge time 13 μs

When the initial concentration increases tenfold, the distribution changes extensively. The direction of the longitudinal component is the same as of the plasma flow in the entire plasma volume (Fig. 6), as opposed to the previous cases. Then, during the discharge, the specific distribution appears indicating the deceleration process (Fig. 7), excluding a small part of the flow where the Ampere force is directed towards the wall of the vacuum chamber.

Acknowledgements

This work has been performed in part within joint projects supported by National Academy of Sciences of Ukraine (NASU) and National Academy of Sciences of Belarus the project № 08-01-18 and the Targeted Program of NASU on Plasma Physics № П-5/24-2018.

References

[1] Morozov A.I. and Solov'ev L.S. 1974 Reviews of Plasma Physics vol. 8 ed. M.A. Leontovich
[2] Solyakov D.G. et al. 2013 Plasma Phys. Rep. 39 986–92
[3] Solyakov D.G. et al. 2012 Plasma Phys. Rep. 38 110–5
[4] Marchenko A.K. et al. 2014 Probl. Atom. Sci. Techn. №6(94), Series: Plasma Physics, p. 83-86
[5] Cherednychenko T.M. et al. 2013 Acta Polytechnica 53(2) 131-133
[6] Garkusha I.E. et al. 2014 Physica Scripta p. 014037
[7] Ladygina M.S. et al. 2016 Physica Scripta p. 074006
[8] Solyakov D.G. et al. 2018 Probl. Atom. Sci. Techn. №6(118), Series: Plasma Physics, p. 130-133
[9] Volkova Y.E. et al. 2017 IEEE Young Scientists Forum p. 134
[10] Astashinskii V.M. et al. 2011 J. Eng. Phys. Therm. 84 1102–7
[11] Astashinskii V.M. et al. 1992 Sov. J. Plasma Phys. 18 47–53